Sampled-data Controller Design with Application to the Quanser AERO 2-DOF Helicopter

Adriano N.D. Lopes, Laurent Arcèse, Kevin Guelton, Abdelmadjid Cherifi

Sampled-data Controller Design with Application to the Quanser AERO 2-DOF Helicopter

Adriano N.D. Lopes*†, Laurent Arcese*, Kevin Guelton* and Abdelmadjid Cherifi*
*CReSTIC EA3804 - Université de Reims Champagne-Ardenne
Moulin de la Housse BP1039, 51100 Reims, France
†Department of Mechatronics Engineering, CEFET-MG - Campus Divinópolis
R. Álvares Azevedo, 400, Divinópolis, 35503-822, MG, Brazil
Emails: {adriano.lopes,laurent.arcese,kevin.guelton,abdelmadjid.cherifi}@univ-reims.fr, adriano@cefetmg.br

***Abstract*—This paper investigates the importance of considering the discrete-time nature of embedded controllers for continuous-time dynamical systems, namely the sampled-data control approach. To illustrate such approach, an experimental study is conducted with the Quanser® AERO platform in its 2-DOF helicopter configuration. New LMI-based conditions are provided for the design of sampled-data controllers for linear systems. These are obtained from the usual Lyapunov-Krasovskii approach and useful bounding techniques. The results are validated in simulation as well as experimentally, with a successful comparison to conventional continuous-time controllers design by Quanser®, especially when the sampling period is high.**

***Index Terms*—Sampled-data controllers, Lyapunov Krasovskii Functionals (LKF), Quanser® AERO, 2-DOF Helicopter.**

I. Introduction

Over the past decades, due to the technological improvements on microprocessors and/or low-cost computers (e.g. Raspberry, BeagleBone, Arduino, etc.), advances in mechatronic devices or embedded systems allow their size reductions, scalability, and the optimization of their energy consumption. In this context, controllers are often implemented in a discrete-time framework when the systems to be controlled may present continuous-time dynamics. Hence, practically speaking, two approaches are usually considered for such controller design: *i)* designing the controllers for the continuous-time systems and directly apply them by assuming that the sampling rate is fast enough to capture as much as possible the plants behavior [1]–[3], *ii)* perform a plant discretization, considering a constant sampling period that preserves as much as possible the system dynamics and then, make the synthesis of a discrete-time controller [4]–[6]. However, it is essential to highlight that with the above mentioned approaches, the inter-sampling behavior of the continuous-time system is not considered, which may leads to instability and/or loss of robustness of the controlled plant, especially when large sampling periods are considered [7]. Furthermore, enlarging the sampling period allows to reduce computational burden and/or energy consumption. Accordingly, to cope with such issues, sampled-data control approaches emerged as a promising research topic in control theory. It consists in the investigation of the overall closed-loop stability of continuous-time plants driven by digital controllers based on sampled-data measurements, see e.g. [7], [8]. To do so, an elegant and powerful way to design such controllers consists in rewriting the closed-loop dynamics as a continuous-time system with input time-varying delay, also known as a time-delay approach for the stabilization of sampled-data systems [8].

In this paper, we are concerned with the real-time application of recent techniques for the design of sampled-data controller on an unmanned aerial vehicles (UAVs) benchmark, which present some interesting characteristics such as its versatility, maneuverability, and ease of use. Namely, we choose for these experiments the Quanser® AERO benchmark configured as a dual-rotor helicopter [9]. For this real system, some works can be found in the literature dealing with reinforcement learning strategies [10], model reference adaptive controllers [2], [3] and robust controllers [1], [11], [12]. Nevertheless, all the above mentioned works assume continuous-time behaviour of the controller part and, to the best of the authors knowledge, no previous studies can be found dealing with the design of a sampled-data controller for this system.

This paper presents new design conditions for sampled-data controllers dedicated to stabilize continuous-time linear systems. It follows a recent study dedicated to the conservatism reduction in the Takagi-Sugeno model-based framework [13], by providing real-time experimental validation of the proposed sampled-data controller design procedure. The effectiveness of this proposal is illustrated in simulation, then validated experimentally, and compared to conventional continuous-time PID and LQR controllers, which design procedure can be found in the Quanser® AERO laboratory guide [9].

Notations. Stars * in symmetric matrices denote block transpose quantities. We denote the set of integers $\mathcal{I}_r = \{1, ..., r\}$. For any matrix M, $\mathcal{H}(M) = M + M^T$. I is an identity matrix with appropriate dimension. For vectors v_1, v_2,..., v_n, $col\{v_1, v_2, ..., v_n\} = \begin{bmatrix} v_1^T & v_2^T & \dots & v_n^T \end{bmatrix}^T$.

II. Quanser®AERO Model and Preliminaries on Sampled-data Control

In this section, we first present the dynamical model of the Quanser®AERO in its 2-DOF Helicopter configuration, then useful lemmas to derive the design conditions proposed in section III.

A. 2-DOF helicopter dynamical model

Figure 1 presents the free-body diagram of the considered Quanser®AERO benchmark.

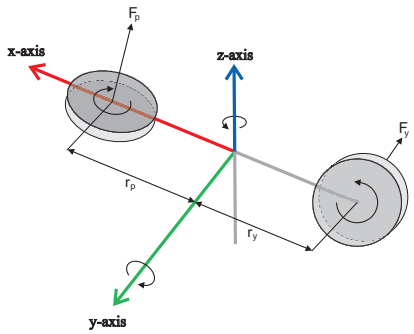

Fig. 1. Simple free-body diagram of a 2-DOF helicopter system.

This system is configured as a conventional dual-rotor helicopter with two identical high-efficiency rotors that produce the thrust forces $F_p(t)$ and $F_y(t)$ acting at points with distances r_p and r_y from the *z-axis* along the *x-axis*, respectively. Hence, one propeller generates a torque around the *y-axis* leading to a pitch ($\theta(t)$) motion, while the other one deals with a yaw ($\psi(t)$) motion (around the *z-axis*). The dynamical model of this benchmark is given by [9]:

$$J_p\ddot{\theta}(t) + D_p\dot{\theta}(t) + K_{sp}\theta = \tau_p(t) \quad (1)$$

$$J_u\ddot{\psi}(t) + D_y\dot{\psi}(t) = \tau_y(t) \quad (2)$$

with the parameters given in Table 1.

The torques acting on the pitch ($\tau_p(t)$) and yaw ($\tau_y(t)$) axes are assumed proportional to the inputs voltages $V_p(t)$ and $V_y(t)$ of the DC-motors such that:

$$\tau_p(t) = K_{pp}V_p(t) + K_{py}V_y(t) \quad (3)$$

$$\tau_y(t) = K_{yp}V_p(t) + K_{yy}V_y(t) \quad (4)$$

with the parameters also defined in Table 1.

B. State-space model and sampled-data problem statement

Let us consider the state vector $x^T(t) = \begin{bmatrix}\theta(t) & \psi(t) & \dot{\theta}(t) & \dot{\psi}(t)\end{bmatrix}$ and the input vector $u^T(t) = \begin{bmatrix}V_p(t) & V_y(t)\end{bmatrix}$, the linear state-space model of the 2-DOF Helicopter is given by:

$$\dot{x}(t) = Ax(t) + Bu(t) \quad (5)$$

with $A = \begin{bmatrix} 0 & 0 & 1 & 0 \\ 0 & 0 & 0 & 1 \\ -\frac{K_{sp}}{J_p} & 0 & -\frac{D_p}{J_p} & 0 \\ 0 & 0 & 0 & -\frac{D_y}{J_y} \end{bmatrix}, B = \begin{bmatrix} 0 & 0 \\ 0 & 0 \\ \frac{K_{pp}}{J_p} & \frac{K_{py}}{J_p} \\ \frac{K_{yp}}{J_y} & \frac{K_{yy}}{J_y} \end{bmatrix}$.

In this paper, we consider the stabilization of the linear system (5) from the following sampled-data state feedback control law:

$$u(t) = -Fx(t_k) \quad (6)$$

where $K \in \mathbb{R}^{m\times n}$ is the controller gain matrix to be designed and t_k denotes sampling instants.

TABLE I
2-DOF HELICOPTER PARAMETERS

	Parameter	Value	Unit
J_p	Moment of Inertia about the pitch axis	0.0215	$kg.m^2$
J_y	Moment of Inertia about the yaw axis	0.0215	$kg.m^2$
K_{sp}	Stiffness about the pitch axis	0.0374	$N.m/rad$
D_p	Pitch viscous friction constant	0.0071	$N.m.s/rad$
D_y	Yaw viscous friction constant	0.0220	$N.m.s/rad$
K_{pp}	Thrust-torque gain acting on pitch axis from pitch propeller	0.0011	$N.m/V$
K_{yy}	Thrust-torque gain acting on yaw axis from yaw propeller	0.0022	$N.m/V$
K_{py}	Thrust-torque gain acting on pitch axis from yaw propeller	0.0021	$N.m/V$
K_{yp}	Thrust-torque gain acting on yaw axis from pitch propeller	-0.0027	$N.m/V$

A zero holder is applied to maintain $x(t_k)$ during aperiodic inter-sampling intervals $[t_k, t_{k+1})$, with an inner sampling period $\eta_k > 0$ that can be non uniform over samples and with a maximal allowable sampling period $\bar{\eta}$ to be estimated (i.e. $t_{k+1} - t_k \leq \eta_k \leq \bar{\eta}$). In this context, for actual $t \in [t_k, t_{k+1})$, we define $\tau(t) = t - t_k \in [0, \eta_k)$ with $\dot{\tau}(t) = 1$. Hence, the control law (6) can be rewritten as:

$$u(t) = -Fx(t-\tau(t)) \quad (7)$$

then substituting (7) in (5) allows to express the closed-loop dynamics as:

$$\dot{x}(t) = Ax(t) - BFx(t-\tau(t)) \quad (8)$$

Our goal is to design the sampled-data controller gain matrix F with a maximal sampling period $\bar{\eta}$, which guarantee the asymptotic stability of the closed-loop dynamics (8).

C. Useful lemmas

The following lemmas will be considered to derive the sampled-data controller design conditions proposed in the next section.

Lemma 1: [14]: For any constant matrix $R \in \mathbb{R}^{n\times n}$, $R = R^T > 0$, a scalar function $\tau(t)$ with $0 < \tau(t) \leq \tau_M$ and a vector function $\dot{x} : [-\tau_M, 0] \to \mathbb{R}^n$ such that the integration concerned is well defined, let:

$$\int_{t-\tau(t)}^{t} \dot{x}(s)ds = E\psi(t) \quad (9)$$

where $E \in \mathbb{R}^{n\times k}$ and $\psi(t) \in \mathbb{R}^k$. Then the following inequality holds for any matrix $M \in \mathbb{R}^{n\times k}$:

$$-\int_{t-\tau(t)}^{t} \dot{x}^T(s)R\dot{x}(s)ds \leq \psi^T(t)\Upsilon\psi(t) \quad (10)$$

where $\Upsilon = -E^TM - M^TE + \tau(t)M^TR^{-1}M$.

Lemma 2: [15] For any matrix $P = P^T > 0$ with appropriate dimensions, $\tau(t) \in [0, \eta_k)$, the following inequality holds:

$$\int_{t-\tau(t)}^{t} x^T(s)Px(s)ds \geq \eta_k^{-1}\int_{t-\tau(t)}^{t} x^T(s)P\int_{t-\tau(t)}^{t} x(s)ds \quad (11)$$

Lemma 3: [16] Let $\xi \in \mathbb{R}^n$, $G \in \mathbb{R}^{m\times n}$ and $Q = Q^T \in \mathbb{R}^{n\times n}$ such that $rank(G) < n$. The following statements are equivalent.

$$\xi^T Q\xi < 0, \quad \forall \xi \in \{\xi \in \mathbb{R}^n : \xi \neq 0, G\xi = 0\} \tag{12}$$

$$\exists R \in \mathbb{R}^{n\times m} : Q + RG + G^T R^T < 0 \tag{13}$$

III. Main results

In this section LMI-based conditions for the design of sampled-data controllers (6) dedicated to stabilize continuous-time linear systems (1) is provide. The following Theorem summarize the conditions. For the sake of generality, one denotes respectivelly n and m the number of state variables and inputs.

Theorem 1: For aperiodic sampling periods $\eta_k \leq \bar{\eta}$ to be maximized, the linear system (5) is stabilized by the sampled-data controller (6) if there exists the matrices $0 < \bar{L} = \bar{L}^T \in \mathbb{R}^{n\times n}$, $\bar{M} = \bar{M}^T \in \mathbb{R}^{4n\times 4n}$, $0 < \bar{N} = \bar{N}^T \in \mathbb{R}^{n\times n}$, $\bar{P} = \bar{P}^T \in \mathbb{R}^{n\times n}$, $X \in \mathbb{R}^{n\times n}$, $K \in \mathbb{R}^{m\times n}$, $\bar{Y} \in \mathbb{R}^{4n\times n}$, $\bar{U} = \bar{U}^T \in \mathbb{R}^{3n\times 3n}$ and the scalars ε_1, ε_2 and ε_3, such that the following conditions are satisfied:

$$\bar{M}^0 - \bar{U} < 0 \tag{14}$$

$$\bar{\Phi}^0_\Sigma + \mathbb{I}_\varepsilon \bar{G} + \bar{G}^T \mathbb{I}_\varepsilon^T < 0 \tag{15}$$

$$\begin{bmatrix} \eta_k^2 \bar{S} + \eta_k \bar{\Phi}^1_\Sigma + \bar{\Phi}^0_\Sigma + \mathbb{I}_\varepsilon \bar{G} + \bar{G}^T \mathbb{I}_\varepsilon^T & \eta_k \bar{Y}^T & \eta_k \bar{Q}^T \\ \eta_k \bar{Y} & -\eta_k \bar{P} & 0 \\ \eta_k \bar{Q} & 0 & -\bar{U} \end{bmatrix} < 0 \tag{16}$$

$$\mathbb{I}_\varepsilon = \begin{bmatrix} I & \varepsilon_1 I & \varepsilon_2 I & \varepsilon_3 I \end{bmatrix}^T, \bar{Q} = \begin{bmatrix} 0 & \bar{W} \end{bmatrix},$$

$$\bar{G} = \begin{bmatrix} AX & -BK & 0 & -X \end{bmatrix}, \bar{S} = \begin{bmatrix} \bar{U} - \bar{M}^0 & 0 \\ 0 & 0 \end{bmatrix}$$

$$\bar{\Phi}^1_\Sigma = \mathcal{H}\left(\bar{\eta} E_2^T \bar{M} E_3 - E_2^T \bar{M} E_2\right) - \begin{bmatrix} \bar{N} & 0 & 0 & 0 \\ 0 & 0 & 0 & 0 \\ 0 & 0 & 0 & 0 \\ * & 0 & 0 & \bar{P} \end{bmatrix},$$

$$\bar{\Phi}^0_\Sigma = \bar{\eta} E_2^T \bar{M} E_2 - \mathcal{H}\left(E_1^T \bar{Y}\right) + \begin{bmatrix} \bar{\eta}\bar{N} & 0 & 0 & \bar{L} \\ 0 & 0 & 0 & 0 \\ 0 & 0 & -\eta_k^{-1}\bar{N} & 0 \\ * & 0 & 0 & \bar{\eta}\bar{P} \end{bmatrix},$$

$$\bar{M} = \begin{bmatrix} \bar{M}_{11} & \bar{M}_{12} & \bar{M}_{13} & \bar{M}_{14} \\ * & \bar{M}_{22} & \bar{M}_{23} & \bar{M}_{24} \\ * & * & \bar{M}_{33} & \bar{M}_{34} \\ * & * & * & \bar{M}_{44} \end{bmatrix}, \bar{W} = \begin{bmatrix} \mathcal{H}(\bar{M}_{14}) + \bar{M}_{11} + \bar{M}_{44} \\ \bar{M}_{24} - \bar{M}_{44} + \bar{M}_{12}^T - \bar{M}_{14}^T \\ \bar{M}_{34} + \bar{M}_{13}^T \end{bmatrix},$$

$$\bar{M}^0 = \begin{bmatrix} \mathcal{H}(\bar{M}_{13} + \bar{M}_{34}) & \bar{M}_{23}^T - \bar{M}_{34} & \bar{M}_{33}^T \\ * & 0 & 0 \\ * & 0 & 0 \end{bmatrix}, E_1^T = \begin{bmatrix} I \\ -I \\ 0 \\ 0 \end{bmatrix}^T,$$

$$E_2 = \begin{bmatrix} I & 0 & 0 & 0 \\ 0 & I & 0 & 0 \\ 0 & 0 & I & 0 \\ I & -I & 0 & 0 \end{bmatrix}, E_3 = \begin{bmatrix} 0 & 0 & 0 & I \\ 0 & 0 & 0 & 0 \\ I & 0 & 0 & 0 \\ 0 & 0 & 0 & I \end{bmatrix},$$

In that case, the sampled-data gain matrix can be recover by $F = KX^{-1}$.

Proof: Let us consider the following LKF candidate:

$$V(t) = V_1(t) + V_2(t) + V_3(t) + V_4(t) \tag{17}$$

where:

$$V_1(t) = x(t)^T L x(t) \tag{18}$$

$$V_2(t) = (\eta_k - \tau(t)) \int_{t-\tau(t)}^{t} x^T(s) N x(s) ds \tag{19}$$

$$V_3(t) = (\eta_k - \tau(t)) \int_{t-\tau(t)}^{t} \dot{x}^T(s) P \dot{x}(s) ds \tag{20}$$

$$V_4(t) = (\eta_k \tau(t) - \tau^2(t)) \zeta^T(t) M \zeta(t) \tag{21}$$

with $\zeta(t) = col\left\{x(t), x(t-\tau(t)), \int_{t-\tau(t)}^{t} x(s)ds, \int_{t-\tau(t)}^{t} \dot{x}(s)ds\right\}$.

Assuming $L = L^T > 0$, the whole LKF (17) is continuous and positive at each sample time t_k since we have $V_1(t_k) > 0$ and $V_\ell(t_k^-) = V_\ell(t_k) = 0$, for $\ell = 2, ..., 4$. Hence, since the LKF $V(t)$ is continuous $\forall t \in [t_k, t_{k+1})$, if it can be proven to be monotonously decreasing during this interval, then it is positive $\forall t \in [0, +\infty)$ and the closed-loop dynamics (8) is stable. That is to say if, $\forall t \in [t_k, t_{k+1})$:

$$\dot{V}(t) = \dot{V}_1(t) + \dot{V}_2(t) + \dot{V}_3(t) + \dot{V}_4(t) < 0 \tag{22}$$

In the sequel of the proof, the state vector extension $\xi(t) = col\left\{x(t), x(t-\tau(t)), \int_{t-\tau(t)}^{t} x(s)ds \dot{x}(t)\right\}$ is considered. The derivative of $V_1(t)$ can be written as:

$$\dot{V}_1(t) = 2x^T(t) L \dot{x}(t) = \xi^T(t) \Phi_1^0 \xi(t), \Phi_1^0 = \begin{bmatrix} 0 & 0 & 0 & L \\ 0 & 0 & 0 & 0 \\ 0 & 0 & 0 & 0 \\ L & 0 & 0 & 0 \end{bmatrix} \tag{23}$$

Assuming $N > 0$ and applying lemma 2, for the derivative of $V_2(t)$ we can write:

$$\begin{aligned} \dot{V}_2(t) &= (\eta_k - \tau(t)) x^T(t) N x(t) - \int_{t-\tau(t)}^{t} x^T(s) N x(s) ds \\ &\leq (\eta_k - \tau(t)) x^T(t) N x(t) - \eta_k^{-1} \int_{t-\tau(t)}^{t} x^T(s) N \int_{t-\tau(t)}^{t} x(s) ds \\ &= \tau(t) \xi^T(t) \Phi_2^1 \xi(t) + \xi^T(t) \Phi_2^0 \xi(t) \end{aligned} \tag{24}$$

with $\Phi_2^1 = \begin{bmatrix} -N & 0 & 0 & 0 \\ 0 & 0 & 0 & 0 \\ 0 & 0 & 0 & 0 \\ 0 & 0 & 0 & 0 \end{bmatrix}$, $\Phi_2^0 = \begin{bmatrix} \eta_k N & 0 & 0 & 0 \\ 0 & 0 & 0 & 0 \\ 0 & 0 & -\eta_k^{-1} N & 0 \\ 0 & 0 & 0 & 0 \end{bmatrix}$.

It follows, assuming $P > 0$, for the derivative of $V_3(t)$:

$$\dot{V}_3(t) = (\eta_k - \tau(t)) \dot{x}^T(t) P \dot{x}(t) - \int_{t-\tau(t)}^{t} \dot{x}^T(s) P \dot{x}(s) ds \tag{25}$$

Note that $\int_{t-\tau(t)}^{t} \dot{x}^T(s) ds = E_1 \xi(t)$ with $E_1 = \begin{bmatrix} I & -I & 0 & 0 \end{bmatrix}$. From lemma 1, for any matrix Y we can write:

$$\begin{aligned} \dot{V}_3(t) &\leq (\eta_k - \tau(t)) \dot{x}^T(t) P \dot{x}(t) \\ &+ \xi^T(t) \left(-E_1^T Y - Y^T E_1 + \tau(t) Y^T P^{-1} Y\right) \xi(t) \\ &= \tau(t) \xi^T(t) (\Phi_3^1 + Y^T P^{-1} Y) \xi(t) + \xi^T(t) \Phi_3^0 \xi(t) \end{aligned} \tag{26}$$

with $\Phi_3^1 = -\begin{bmatrix} 0 & 0 & 0 & 0 \\ 0 & 0 & 0 & 0 \\ 0 & 0 & 0 & 0 \\ 0 & 0 & 0 & P \end{bmatrix}$ and $\Phi_3^0 = -\mathcal{H}\left(E^T Y\right) + \begin{bmatrix} 0 & 0 & 0 & 0 \\ 0 & 0 & 0 & 0 \\ 0 & 0 & 0 & 0 \\ 0 & 0 & 0 & \eta_k P \end{bmatrix}$.

Finally, with the derivative of $V_4(t)$ we get:

$$\begin{aligned} \dot{V}_4(t) =& (\eta_k - 2\tau(t)) \zeta^T(t) M \zeta(t) \\ &+ 2(\eta_k \tau(t) - \tau^2(t)) \zeta^T(t) M \dot{\zeta}(t) \end{aligned} \tag{27}$$

That is to say, with $\zeta(t) = E_2\xi(t)$ and $\dot{\zeta}(t) = E_3\xi(t)$:

$$\begin{aligned}\dot{V}_4(t) =&\tau^2(t)\xi^T(t)\Phi_4^2\xi(t)\\ &+\tau(t)\xi^T(t)\Phi_4^1\xi(t)+\xi^T(t)\Phi_4^0\xi(t)\end{aligned} \tag{28}$$

where $\Phi_4^2 = -\mathcal{H}\left(E_2^T M\mathbb{E}_2\right)$, $\Phi_4^1 = \mathcal{H}\left(\eta_k E_2^T M E_3 - E_2^T M E_2\right)$ and $\Phi_4^0 = \eta_k E_2^T M E_2$.
Now, considering (23), (24), (26) and (28), the inequality (22) holds if:

$$\begin{aligned}\mathcal{P}(\tau(t)) =&\tau^2(t)\xi^T(t)\Phi_4^2\xi(t)\\ &+\tau(t)\xi^T(t)(\Phi_\Sigma^1 + Y^T P^{-1} Y)\xi(t)\\ &+\xi^T(t)\Phi_\Sigma^0\xi(t) < 0\end{aligned} \tag{29}$$

with $\Phi_\Sigma^1 = \Phi_4^1+\Phi_3^1+\Phi_2^1$ and $\Phi_\Sigma^0 = \Phi_4^0+\Phi_3^0+\Phi_2^0+\Phi_1^0$.
Note that, $\forall\xi(t)$ the convexity of the polynomial $\mathcal{P}(\tau(t)) = 0$ is granted if:

$$\xi^T(t)\Phi_4^2\xi(t) > 0 \quad \Leftrightarrow \quad \Phi_4^2 > 0 \tag{30}$$

In this case, the inequality (29) holds if:

$$\mathcal{P}(0) < 0 \text{ and } \mathcal{P}(\eta_k) < 0 \tag{31}$$

Hence, focusing first on (30), we assume:

$$M = M^T = \begin{bmatrix} M_{11} & M_{12} & M_{13} & M_{14} \\ * & M_{22} & M_{23} & M_{24} \\ * & * & M_{33} & M_{34} \\ * & * & * & M_{44} \end{bmatrix} \tag{32}$$

and, from (28) we can write:

$$\Phi_4^2 = -\begin{bmatrix} M^0 & W \\ * & 0 \end{bmatrix} \tag{33}$$

with $M^0 = \begin{bmatrix} \mathcal{H}(M_{13}+M_{34}) & M_{23}^T - M_{34} & M_{33}^T \\ * & 0 & 0 \\ * & 0 & 0 \end{bmatrix}$,
and $W = \begin{bmatrix} \mathcal{H}(M_{14}) + M_{11} + M_{44} \\ M_{24} - M_{44} + M_{12}^T - M_{14}^T \\ M_{34} + M_{13}^T \end{bmatrix}$.
For any regular matrix $U \in \mathbb{R}^{3n\times 3n}$ we have the null terms $W^T U^{-1} W - W^T U^{-1} W = 0$ and $M^0 - M^0 = 0$, which allows us to write, by the application of the Schur complement:

$$\begin{bmatrix} U - M^0 + M^0 & W \\ W^T & W^T U^{-1} W \end{bmatrix} = 0 \tag{34}$$

And so, we can write:

$$\Phi_4^2 = -\begin{bmatrix} M^0 & W \\ W^T & 0 \end{bmatrix} = S + Q^T U^{-1} Q \tag{35}$$

with $S = \begin{bmatrix} U - M^0 & 0 \\ 0 & 0 \end{bmatrix}$ and $Q = [0 \quad W]$.
In the sequel, we substitute the right-hand side of (35) as Φ_4^2 in (29), so the inequality (30) holds if:

$$U > 0 \text{ and } U - M^0 > 0 \tag{36}$$

Now, we need to introduce the closed-loop dynamics in the stability conditions. To do so, let us rewrite (8) as:

$$G\xi(t) = 0 \tag{37}$$

with $G = \begin{bmatrix} A & -BF & 0 & -I \end{bmatrix}$.
Furthermore, (29) can be rewritten as:

$$\xi^T(t)\left(\tau^2(t)\Phi_4^2 + \tau(t)(\Phi_\Sigma^1 + Y^T P^{-1} Y) + \Phi_\Sigma^0\right)\xi(t) < 0 \tag{38}$$

From lemma 3, the inequality (38) holds if there exists $R \in \mathbb{R}^{4n\times n}$ such that:

$$\tau^2(t)\Phi_4^2 + \tau(t)(\Phi_\Sigma^1 + Y^T P^{-1} Y) + \Phi_\Sigma^0 + RG + G^T R^T < 0 \tag{39}$$

From (31), the inequality (39) hold if both the following inequalities holds:

$$\Phi_\Sigma^0 + RG + G^T R^T < 0 \tag{40}$$

$$\eta_k^2\Phi_4^2 + \eta_k(\Phi_\Sigma^1 + Y^T P^{-1} Y) + \Phi_\Sigma^0 + RG + G^T R^T < 0 \tag{41}$$

Considering the right-hand side of (35) as Φ_4^2, then applying the Schur complement on (41), we get:

$$\begin{bmatrix} \eta_k^2 S + \eta_k\Phi_\Sigma^1 + \Phi_\Sigma^0 + RG + G^T R^T & \eta_k Y^T & \eta_k Q^T \\ \eta_k Y & -\eta_k P & 0 \\ \eta_k Q & 0 & -U \end{bmatrix} < 0 \tag{42}$$

Assuming $R = \begin{bmatrix} X^{-1} & \varepsilon_1 X^{-1} & \varepsilon_2 X^{-1} & \varepsilon_3 X^{-1} \end{bmatrix}^T$, with X a regular matrix, then pre- and post-multiplying (40) respectively by $D_X^T = diag\begin{bmatrix} X & X & X & X \end{bmatrix}^T$ and its transpose, we get (15). Similarly, pre- and post-multiplying (42) respectively by $D_X^T = diag\begin{bmatrix} X & X & X & X & X & X & X & X \end{bmatrix}^T$ and its transpose, we get (16). Where $\mathbb{I}_\varepsilon = \begin{bmatrix} I & \varepsilon_1 I & \varepsilon_2 I & \varepsilon_3 I \end{bmatrix}^T$, $\bar{G} = \begin{bmatrix} AX & -BK & 0 & -X \end{bmatrix}$, $K = FX$, and all decision matrices inside $\bar{\Phi}_4^2$, $\bar{\Phi}_\Sigma^1$ and $\bar{\Phi}_\Sigma^0$ are rewritten with the bijective change of variables $\bar{D} = X^T D X$ ($D = \{L, M_{11}, \ldots, M_{44}, N, P, U\}$). ■

Remark 1: Because of the parameters ε_1, ε_2 and ε_3, The conditions presented in Theorem 1 are not strictly LMI. However, as stated in many previous works applying the Finsler's lemma, see e.g. [13], [17]–[21], these parameters help to significantly improve the conservatism of the conditions and can be, as usual, tuned offline by grid search. This allows to reach a large value of $\bar{\eta}$ in the considered context of sampled-data control.

IV. Simulation and Experimental Results

In this section, simulation and experimental results are provided to illustrate the usefulness of the proposed sample-data controller design regarding to the conventional continuous-time methodologies, namely Proportional-Derivative (PD) and LQR controllers design, proposed by the Quanser® team in the AERO Laboratory Guide [9], when large enough sampling periods are considered for the embedded controller.

A. Overview on the control approaches proposed in Quanser®AERO laboratory guide

First, based on the standard linear control theory for SISO systems, decoupled PD control laws are proposed for the the pitch and yaw axis as:

$$\begin{aligned}u_\theta(t) &= -K_{P_p}\theta(t) - K_{D_p}\dot{\theta}(t)\\ u_\psi(t) &= -K_{P_y}\psi(t) - K_{D_y}\dot{\psi}(t)\end{aligned} \tag{43}$$

with the gains $K_{P_p} = 107.7148$, $K_{D_p} = 52.4365$, $K_{P_y} = 54.1163$ and $K_{D_y} = 19.5924$, designed from standard decoupled second-order transfer functions models and some performances index based on the natural frequency w_n, damping ratio ζ, peak time t_p and overshoot specification P_O (see the Quanser®AERO laboratory guide [9] for more details).

Then, based on the fact that the above mentioned PD controllers doesn't cope with coupling effects, the following linear state feedback controller is considered:

$$u(t) = -K_{LQR}x(t), \tag{44}$$

Its design is proposed in [9] from the LQR approach considering the minimization of the following cost function:

$$J(u(t)) = \int_0^\infty \left(x(t)^T Q x(t) + u(t)^T R u(t)\right) dt \tag{45}$$

with $Q = \begin{bmatrix} 200 & 0 & 0 & 0 \\ 0 & 75 & 0 & 0 \\ 0 & 0 & 0 & 0 \\ 0 & 0 & 0 & 0 \end{bmatrix}$ and $R = \begin{bmatrix} 0.005 & 0 \\ 0 & 0.005 \end{bmatrix}$, which provides the following gain matrix:

$$K_{LQR} = \begin{bmatrix} 98.2088 & -103.0645 & 32.2643 & -29.0750 \\ 156.3469 & 66.1643 & 45.5122 & 17.1068 \end{bmatrix}$$

Let us highlight that these controllers are projected in continuous-time and are implemented in the Quanser® lab assuming a very small sampling period ($\eta_k = 2ms$), which is satisfactory for a pedagogical tool to teach basics on this topics. Nevertheless, since the embedded electronics of the Quanser®AERO provides only digital computations, from the theoretical point of view, this is not accurate since the inter-sampling stability is not guarantee in these two cases, especially for large sampling periods as illustrate in the next subsections.

B. Simulation results with a large sampling period

In this section, we provide some simulation results considering a large sampling period of $\bar{\eta} = 4.5s$. In this case, solving the conditions of Theorem 1 with YALMIP and SEDUMI in the MATLAB framework, setting $\epsilon_1 = 3$, $\epsilon_2 = 1$ and $\epsilon_3 = 300$, we obtain the following sampled-data control gain for (7):

$$F = \begin{bmatrix} -0.0432 & -1.1617 & 0.1687 & 0.1789 \\ -0.0530 & 0.6085 & 0.2070 & -0.0937 \end{bmatrix}$$

Fig. 2 shows the closed-loop continuous-time responses of the pitch and yaw axis under the design sampled-data control law with the initial conditions $x(0) = \begin{bmatrix} 10 & 45 & 0 & 0 \end{bmatrix}^T$. We can notice that the closed-loop sampled-data systems is successfully stabilized in simulation.

Now, let us consider that the continuous-time controllers (43) and (44) are implemented on a digital device with the same huge sampling period of $4.5s$. As mentioned above, since these controller doesn't cope with inter-sampling behaviour, the closed-loop systems are unstable as shown in the simulations depicted in Fig. 3.

These simulations confirm the significance of the proposed sampled-data control methodology for large sampling periods. The next section provides an experimental validation.

C. Experimental validation of the proposed sampled-data controller design methodology

In the previous subsection, simulation results of the proposed sampled-data control strategy has been proposed with a large sampling period of $4.5s$. Nevertheless, in practice, some

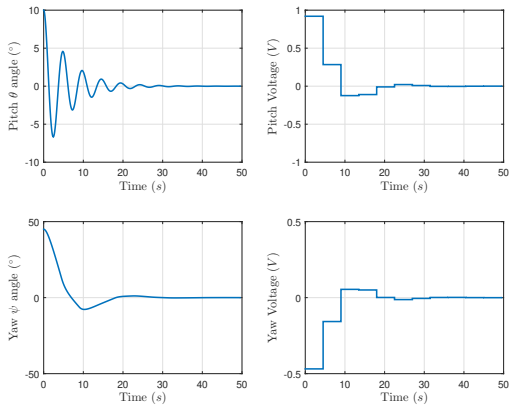

Fig. 2. Time response of Quanser®AERO model under the Sampled Data Controller.

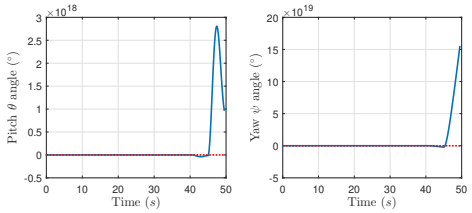

Fig. 3. Time response of Quanser®AERO model, subjected to a LQR Controller (—) and PD Controller (· · ·) under a sampling period of $4.5s$.

unmodeled phenomena (frictions, motors dead zone which make then static under a tension smaller than 0.4V,...) does not allow a direct implementation with the same values. Hence, to provide a fair comparison with a realistic sampling period, we chose for experimental validation $\eta_k = 150ms$. In this case, Theorem 1 have a solution with $\epsilon_1 = 0.25$, $\epsilon_2 = 10$ and $\epsilon_3 = 0.37$, which provide the following sampled-data controller (7) gain matrix:

$$F = \begin{bmatrix} 28.4589 & -34.6979 & 27.5479 & -21.9293 \\ 34.9268 & 18.1751 & 33.8088 & 11.4868 \end{bmatrix}$$

The experimental results are shown in Fig. 4 where the time response and the input signals (Motors' voltage) are depicted for the PD, the LQR and the sampled-data controller. We can notice that, while the PD and LQR control plants that are unstable with a sampling period $\eta_k = 150ms$, the sampled-data controller successfully stabilizes the Quanser®AERO.

Finally, to take benefit of the fact that our conditions hold for aperiodic sampling periods, we proposed the following strategy to trigger it. Note that $V_1(t_k) \leq V_1(0)$. The purpose is to update the sampling period η_k at each sampling instant t_k so that, when $V_1(t_k)$ is closed to $V_1(0)$, then the updated sampling period η_k is small ($2ms$), and when it is close to 0, then η_k is large ($0.15s$). This can be achieved by implementing the simple rule $\eta_k = \frac{0.002-0.15}{V_1(0)} V_1(t_k) + 0.15$. Fig. 5 compares the simulation results with the experimental ones under the proposed aperiodic sampled-data control scheme. As expected, the closed-loop system is properly stabilized. However, we can see some differences during the transients from the simulation and the experimentation. Indeed, these are due to the actuators

saturation, which occurs in practice and which is not taken into account in the present controller design methodology. This will be the subject of our future prospects.

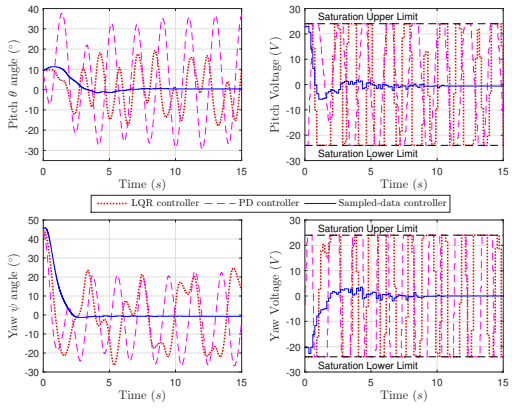

Fig. 4. Comparison of the time responses of the Quanser® AERO under a sampling period of $150ms$.

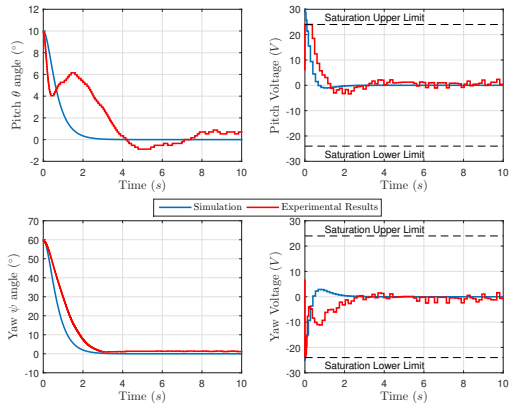

Fig. 5. Time responses of the Quanser® AERO under triggered sampling period.

V. Conclusion

In this paper, the design and the implementation of a sampled-data controller for the Quanser® AERO 2-DOF helicopter system has been proposed. The sampled-data controller design has been achieved from LMI-based conditions obtained from the choice of a convenient LKF and bounding techniques. The results have been validated in simulation as well as experimentally and the designed sampled-data controller shown its superiority regarding to previous designed continuous-time controllers from the Quanser® AERO laboratory guide, especially for large sampling periods. Our further prospects will focus on taking into account actuators saturation in the design conditions as well as to deal with the tracking sampled-data control.

Acknowledgment

The authors would like to thank Mr Eli Kopter for the inspiration he draws to this study. This work is partially funded by the Region Grand-Est, France, with the CPER FFCA Project.

References

[1] A. AlHamouch, M. Tuqan, C. Bardawil, and N. Daher, "Investigating performance of adaptive and robust control schemes for quanser aero," in *2019 Fourth International Conference on Advances in Computational Tools for Engineering Applications (ACTEA)*, July 2019, pp. 1–6.

[2] E. Arabi and T. Yucelen, "A set-theoretic model reference adaptive control architecture with dead-zone effect," *Control Engineering Practice*, vol. 89, pp. 12 – 29, 2019.

[3] ——, "Experimental results with the set-theoretic model reference adaptive control architecture on an aerospace testbed," in *AIAA Scitech 2019 Forum*, 2019, p. 0930.

[4] M. Hernandez-Gonzalez, A. Alanis, and E. Hernandez-Vargas, "Decentralized discrete-time neural control for a quanser 2-dof helicopter," *Applied Soft Computing*, vol. 12, no. 8, pp. 2462 – 2469, 2012.

[5] A. N. D. Lopes, L. F. S. Valter J. S. Leite, and K. Guelton, "Anti-windup TS Fuzzy PI-like Control for Discrete-Time Nonlinear Systems with Saturated Actuators," *International Journal of Fuzzy Systems*, vol. 22, no. 1, pp. 46–61, 2020.

[6] L. F. P. Silva, V. J. S. Leite, E. B. Castelan, M. Klug, and K. Guelton, "Local stabilization of nonlinear discrete-time systems with time-varying delay in the states and saturating actuators," *Information Sciences*, no. 518, pp. 272–285, 2020.

[7] L. Hetel, C. Fiter, H. Omran, A. Seuret, E. Fridman, J.-P. Richard, and S. I. Niculescu, "Recent developments on the stability of systems with aperiodic sampling: An overview," *Automatica*, vol. 76, pp. 309–335, 2017.

[8] E. Fridman, A. Seuret, and J.-P. Richard, "Robust sampled-data stabilization of linear systems: an input delay approach," *Automatica*, vol. 40, no. 8, p. 1441–1446, 2004.

[9] Quanser. (2016) Quanser aero user manual. [Online]. Available: https://www.quanser.com/products/quanser-aero/

[10] A. Fandel, A. Birge, and S. Miah, "Development of reinforcement learning algorithm for 2-dof helicopter model," in *2018 IEEE 27th International Symposium on Industrial Electronics (ISIE)*, June 2018, pp. 553–558.

[11] R. G. Subramanian and V. K. Elumalai, "Robust mrac augmented baseline lqr for tracking control of 2 dof helicopter," *Robotics and Autonomous Systems*, vol. 86, pp. 70 – 77, 2016.

[12] A. Steinbusch and M. Reyhanoglu, "Robust nonlinear tracking control of a 2-dof helicopter system," in *2019 12th Asian Control Conference (ASCC)*, June 2019, pp. 1649–1654.

[13] A. N. D. Lopes, K. Guelton, L. Arcese, V. J. S. Leite, and F. Bourahala, "Finsler-based sampled-data controller design for Takagi-Sugeno systems," in *21th IFAC World Congress (IFAC 2020)*, July 2020.

[14] X.-M. Zhang and Q.-L. Han, "Novel delay-derivative-dependent stability criteria using new bounding techniques," *International Journal of Robust and Nonlinear Control*, vol. 23, no. 13, pp. 1419–1432, 2013.

[15] E. Fridman, "Tutorial on lyapunov-based methods for time-delay systems," *European Journal of Control*, vol. 20, no. 6, pp. 271 – 283, 2014.

[16] R. Skelton, T. Iwasaki, and K. Grigoriadis, *A unified algebraic approach to linear control design*. Taylor and Francis, London, 1998.

[17] R. C. L. F. Oliveira, M. C. de Oliveira, and P. L. D. Peres, "Robust state feedback lmi methods for continuous-time linear systems: Discussions, extensions and numerical comparisons," in *2011 IEEE International Symposium on Computer-Aided Control System Design (CACSD)*, Sep. 2011, pp. 1038–1043.

[18] F. Bourahala, K. Guelton, N. Manamanni, and F. Khaber, "Relaxed Controller Design Conditions for Takagi–Sugeno Systems with State Time-Varying Delays," *International Journal of Fuzzy Systems*, vol. 19, no. 5, pp. 1406–1416, Oct 2017.

[19] A. Cherifi, K. Guelton, and L. Arcese, "Uncertain TS model-based robust controller design with D-stability constraints—A simulation study of quadrotor attitude stabilization," *Engineering Applications of Artificial Intelligence*, vol. 67, pp. 419–429, 2018.

[20] A. Cherifi, K. Guelton, L. Arcese, and V. J. Leite, "Global non-quadratic d-stabilization of takagi–sugeno systems with piecewise continuous membership functions," *Applied Mathematics and Computation*, vol. 351, pp. 23–36, 2019.

[21] F. Bourahala, K. Guelton, and A. N. Lopes, "Relaxed non-quadratic stability conditions for takagi-sugeno systems with time-varying delays: A wirtinger's inequalities approach," in *2019 IEEE International Conference on Fuzzy Systems (FUZZ-IEEE)*, June 2019.